Validation of State-of-the-Art LES Modelling for Soot Prediction in Rich Premixed Turbulent Flames: a Focus on Oxidation Processes

Aurora Maffina, Sébastien Candel, Benedetta Franzelli

Validation of State-of-the-Art LES Modelling for Soot Prediction in Rich Premixed Turbulent Flames: a Focus on Oxidation Processes

A. Maffina[1], S. Candel[1], and B. Franzelli*[1]

[1]Laboratoire EM2C, CNRS, CentraleSupélec, Université Paris-Saclay, Gif-sur-Yvette, France

Abstract

The availability of large eddy simulations (LES) models for the prediction of soot production in complex configurations is essential to the design of the new generation of combustion systems. This requires a good understanding of the processes leading to soot production and the development and validation of the corresponding models. This motivates the present calculations carried out for a laboratory scale burner (EM2Soot) designed at the EM2C laboratory to study soot production in turbulent swirled flames operating under fully-premixed rich conditions. The laser induced incandescence (LII) imaging data for the soot volume fraction (SVF) are used to test the validity of state-of-the-art numerical LES models for soot prediction. The retained models aim at achieving a good level of accuracy for a reasonable computational cost. The gaseous species kinetics is described with an analytically-reduced chemistry approach while the soot solid phase is computed using a three-equation model. This numerical strategy qualitatively reproduces the SVF in laminar premixed flames. In the considered turbulent burner, the numerical strategy captures the SVF spatial distribution but the predicted yield is notably overestimated with respect to the LII results. An extensive analysis of the flame structure as well as of the soot source terms indicates that this is due to an underestimation of soot oxidation reactions. A parametric study on rich laminar and turbulent flames is then carried out to examine the effect of soot oxidation model on the SVF prediction. This indicates that it is worth testing soot models in turbulent flame conditions to examine their capacities and reveal their shortcomings. It is also concluded that the EMSoot configuration offers an interesting situation for developing and validating soot oxidation models.

Keywords: combustion, soot modeling, LES simulations, gas turbine

Introduction

Soot emissions contribute to air pollution, intervene in climate change processes, and have harmful effects on human health and most notably on the respiratory system [1, 2]. Control and reduction of soot emissions from combustion is then of considerable importance. This requires an understanding of soot formation processes and of the underlying factors. Much knowledge has been accumulated through large scale research efforts including experimentation, modeling and simulation. Investigations have often been focused on chemical kinetics and laminar flames. More recent studies have concerned soot formation in turbulent flames with notable progress in experimentation relying on laser imaging diagnostics (like Laser Induced Incandescence, LII and laser induced fluorescence of soot precursors) [3–6] and in simulation, mainly through DNS and more recently through Large Eddy Simulations (LES) [7–11].

The present contribution is intended to advance the latter simulation tools by making use of data collected in rich premixed laminar flames and in an experiment on rich premixed turbulent flames carried out in the EM2Soot burner designed at the EM2C laboratory. This configuration has provided insights on soot formation and its dependency on three operating parameters that can be independently controlled, namely premixed flame power, mixture equivalence ratio and temperature along the external walls of the chamber. Large Eddy Simulations (LES) have been performed to investigate the observed trends as a function of equivalence ratiov It was shown in that reference that soot production was qualitatively captured in terms of spatial distribution and evolution with respect to the equivalence ratio. The models retained in the calculations were also found to suitably reproduce soot volume fractions in rich laminar premixed flames, but it was also found that the soot volume fraction yield was overestimated in the rich premixed turbulent flame configuration EM2Soot.

The present investigation pursues this effort with the aim of improving the modeling and its validation by specifically focusing on the soot oxidation processes and employing the EM2Soot configuration as a testbed for model assessment and validation. This article begins with a short presentation of the two considered test cases, the first corresponds to a rich premixed laminar flame while the second is a rich premixed turbulent flame formed in the EM2Soot burner. The numerical setup is then briefly presented together with the modeling strategy. Calculations carried out with a reference soot oxidation model are then reported for the two test cases. It is shown that the soot volume fraction is well retrieved in the rich laminar flame case and that the trends observed in the turbulent case are well obtained but that the level of soot is notably overestimated. It is

*Corresponding author: benedetta.franzelli@centralesupelec.fr

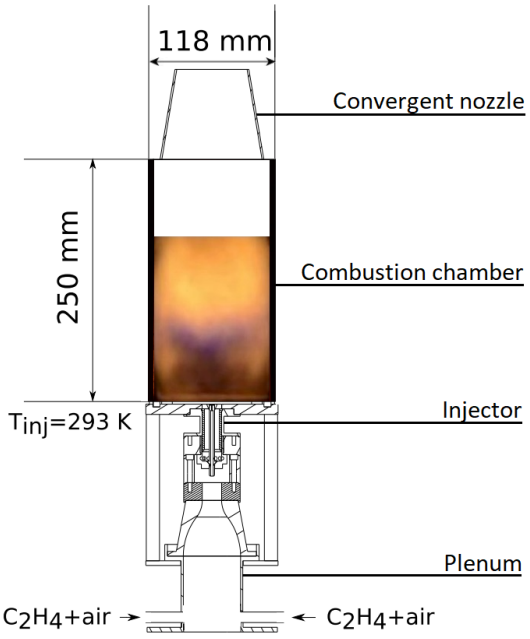

Figure 1: Schematic of the EM2Soot burner (top) and of the injector (bottom). The flame luminosity in the top image corresponds to reference operating conditions: wall temperature $T_c = 690$ K, equivalence ratio $\phi = 1.85$, and premixed flame power $\mathscr{P}_{\text{prem}}$=16.2 kW.

inferred that the source of this discrepancy lies in the soot oxidation modeling. This idea is explored in the final section by augmenting the oxydation rates in the model. This is first tested in the laminar case and then discussed in the rich premixed turbulent case.

Flame configurations

Two different configurations are considered in this work to characterized soot production. On the one side, 1D laminar freely-propagating premixed flames are simulated to validate the numerical models with experiments and to analyse soot production in simple cases. On the other side, the EM2Soot burner allows to investigate soot production in a perfectly premixed swirled turbulent flame. The EM2Soot combustor is fed with a mixture of ethylene and air that is prepared in the upstream manifold and conveyed to a plenum that guarantees a uniform mixing of the flow (Fig. 1). Subsequently, the fuel and oxidizer are injected into the combustion chamber through a radially-swirled injector with swirl number of 0.7. The chamber has a square cross section of 118 × 118 mm^2 and a height of 250 mm. The system works at atmospheric pressure. To avoid backflow of ambient air into the system, a convergent nozzle is placed at the exit of the combustion chamber to accelerate the flow and also to stabilize an external diffusion flame formed by the unburnt products of the rich premixed flame. The length of the combustion chamber and of the exhaust nozzle are such that the external flame has no influence on the combustion process in the chamber [13]. An available experimental dataset featuring different measurements of the flames in the EM2Soot burner is used as a benchmark for the validation of numerical simulations [13]. To observe the flame reaction zone and soot volume fraction, a digital camera captures the flame luminosity, with the blue light indicating the position of the flame reaction zone, and the yellow light indicating soot presence [14]. Laser Induced Incandescence (LII) images of soot volume fraction are available for the first 150 mm of the chamber [14].

Numerical setup

The AVBP CFD solver developed at Cerfacs is used for both sets of numerical calculations: 1D laminar flames and 3D turbulent flames. The gas phase kinetics is represented by the analytically-reduced model C2H4_28_205_14_LG developed for ethylene-air combustion [15]. This scheme includes 28 transported species, 205 reactions and 14 quasi-steady state (QSS) species. The largest gaseous soot precursor is naphthalene (A2), a polycyclic aromatic hydrocarbon with two aromatic rings. Even if larger PAHs are responsible for the formation of solid soot primary particles [16, 17], in the present study, being A2 the largest PAH available, it is the species considered for the onset of nucleation of soot particles. An Eulerian framework in which three equations transport the moment of three global quantities is included to represent the solid phase [18]. The resolved quantities comprising the total number of soot particles N_s, the soot mass fraction Y_s, and the total soot surface S_s are used to obtain other variables of interest for the study of soot production. Using the gas density ρ and the soot particle density $\rho_s = 1.86 \cdot 10^3\, kg/m^3$, it is possible to determine the soot volume fraction starting from the soot mass fraction as follows: $f_v = (\rho/\rho_s)Y_s$. Other than nucleation from A2, the model for the solid phase transformation also includes coagulation, PAH condensation, surface growth via C_2H_2, and oxidation via OH and O_2.

The 1D laminar freely-propagating premixed flames are simulated using a grid with a spatial resolution of

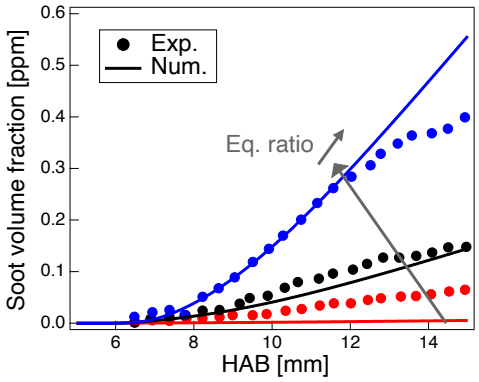

Figure 2: Comparison between experimental [20] and numerical soot volume fraction f_v in a laminar premixed flame at ambient temperature and atmospheric pressure for different values of ϕ.

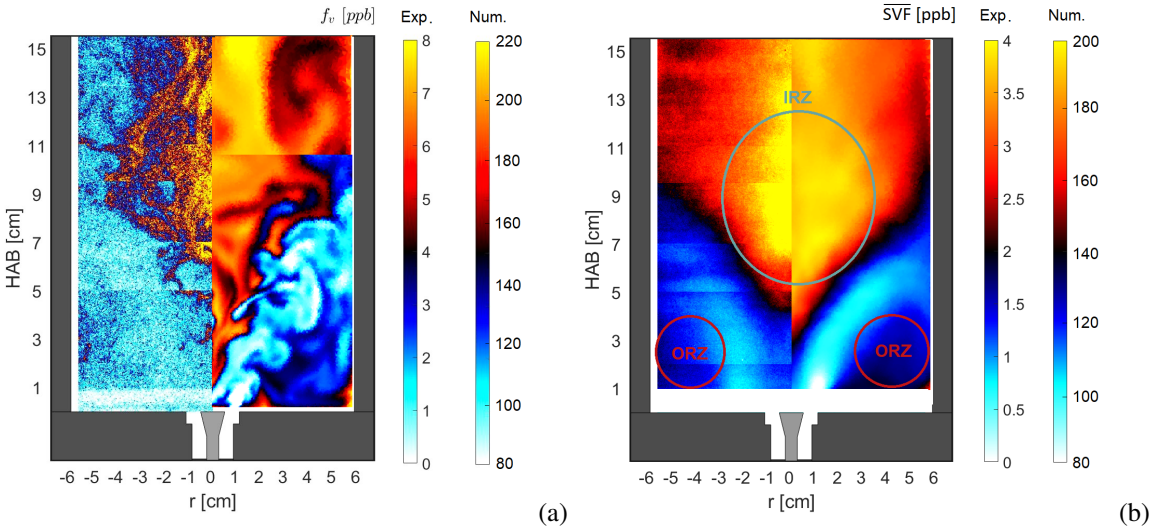

Figure 3: Comparison between experimental (left) and numerical (right) instantaneous (a) and time-averaged (b) SVF at reference conditions [12].

$50\mu m$. The profiles are scaled at x= 5 mm where temperature is equal to 700 K.

The computational domain for the 3D analysis of the EM2Soot case includes the plenum, injector and combustion chamber but the converging nozzle at burner exit is replaced by a straight duct with a length of 100 mm. To avoid backflow from the outlet into the combustion chamber, part of the external atmosphere is included in the model with dimensions of 400 × 400 × 450 mm^3. An LES framework is used to simulate the EM2Soot burner due to its capacity to accurately represent turbulent flows for a CPU cost that is much lower than that required by DNS. This framework together with a relatively coarse grid, is needed to perform parametric studies for a relatively low amount of computational resources. The LES does not account for interactions between the flame and subgrid scales of turbulence. However, since the Reynolds number is relatively low ($Re \simeq 2\ 10^4$), it is expected that these interactions will have a limited impact. The turbulent flow is modeled using the Smagorinsky sub-grid model [19]. Neither the gaseous nor the solid phase includes a turbulent combustion model. This choice is legitimated by the relatively thick flame structure and soot distribution.

The computational grid features around 8.7 million cells. The mesh is refined in the lower part of the chamber, particularly in the injection and reaction regions, with a typical cell size of Δ=0.35 mm. It has been verified that this provides a sufficient number of points to resolve the source terms for gaseous and solid quantities. In fact, at least five points are present in the turbulent flame thickness, that is $\delta_t \approx 2-3.5$ mm based on heat release rate. The 3D calculations adopt a second-order in space and in time numerical scheme to solve the flame over a period of 700 ms. The following results for the EM2Soot burner are obtained at reference wall temperature $T_c = 690$ K, equivalence ratio $\phi = 1.85$, and premixed flame power $\mathscr{P}_{\text{prem}}$=16.2 kW. The time-averaged results are deduced from the last 100 ms, which corresponds to approximately 225 000 CPU hours on an Intel Skylake machine.

Calculations with a reference oxidation model

Laminar flames

The soot models used in the present calculations are essentially validated in laminar flame cases, as illustrated in Fig. 2.

The spatial evolution of the soot volume fraction at various equivalence ratios is compared to experimental results obtained in [20] for wall-stabilized premixed flames. The agreement is quite good. However, experimental results are not available for the equivalence ratio of interest (ϕ=1.85). This is most likely due to the fact that the laminar flame is not producing a significant amount of f_v. The numerical simulation predicts a maximum f_v of the order of 0.1 ppt in the laminar flame case.

EM2Soot case

As can be seen in Fig. 3, the numerical model is able to correctly reproduce the qualitative distribution of soot volume fraction in the EM2Soot combustion chamber both in the instantaneous and time-averaged fields. The instantaneous fields show the presence of ligamentary structures of soot that are wrinkled by the large eddies of the turbulent flow. These structures are well captured by the simulation. Compared to soot production in non-premixed configurations of turbulent jets or swirling flows, soot production is not highly intermittent since under perfectly rich premixed combustion the local conditions are generally favorable to soot formation. Both experimental and numerical data show the macroscopic flow pattern with two recirculation zones: the inner recirculation zone (IRZ) above the reaction zone and around the central axis of the chamber, and the outer recirculation zone (ORZ) in the external part

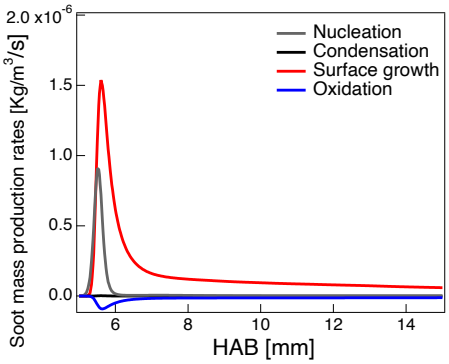

Figure 4: Spatial evolution of soot mass production rate in a laminar premixed flame at ambient temperature and atmospheric pressure for ϕ=1.85.

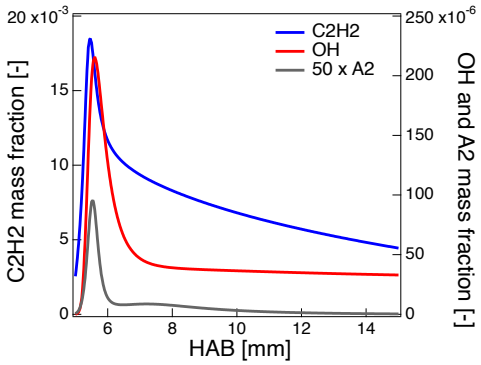

Figure 5: Spatial evolution of C_2H_2, OH and A_2 mass fractions in a laminar premixed flame at ambient temperature and atmospheric pressure for ϕ=1.85.

of the chamber backplane. Even if the qualitative features are correctly reproduced by the simulations, the numerical model leads to an overestimation of the SVF level of two orders of magnitude. This overestimation is observed both in the instantaneous and time-averaged values indicating that this is not due to a possible incorrect prediction of the intermittency. To understand such discrepancies, laminar and turbulent results will be compared in the following.

Comparing laminar and turbulent cases

The numerical simulation predicts a maximum f_v of the order of 0.1 ppt in the laminar flame case at $\phi = 1.85$. This value is much smaller than the instantaneous yield observed experimentally in the EM2Soot case ($\approx$ 8 ppb) and predicted numerically ($\approx$ 200 ppb).

The spatial profiles of some gaseous species of relevance for soot processes (PAHs, OH, C_2H_2) and the source terms that contribute to soot volume fraction (nucleation, condensation, surface growth and oxidation) are displayed in Figs. 4 and 5 for the laminar flame. The observed levels can be compared to the instantaneous fields for the EM2Soot burner in Figs. 6 and 7. One observes that the A_2 mass fraction is significantly higher in the EM2Soot burner compared to that found in the laminar flame. This is probably due to the existence in the EM2Soot system of conditions that favor PAH growth. More precisely, the EM2Soot burner presents an inner recirculation zone (IRZ) characterized by long residence times and temperatures of the order of 1800 K. These temperatures are smaller than the adiabatic flame temperature of the laminar flame because of the non-adiabatic conditions at the combustor walls. This temperature corresponds to the zone of high production of A_2. Due to the long residence times in the IRZ where the temperature has an intermediate value, a higher A_2 mass fraction is observed in the EM2Soot burner. This leads to an enhanced nucleation and condensation of soot particles in the EM2Soot burner compared to the laminar flame augmenting their number and their size. The surface reaction processes, i.e. growth and oxidation, are enhanced as well, finally explaining the differences between laminar and turbulent swirled flames. Even if a higher level of f_v in the EM2Soot burner can be explained, it also appears that the numerical prediction notably overestimates the experimental value. This may have multiple causes: the absence of a subgrid combustion models for gaseous and solid species, the use of a relatively coarse grid, errors in the modelling of the precursors species and/or of soot formation processes.

Among these sources of errors, subgrid models are not expected to affect soot production in the large structures that are suitably resolved on the grid. Concerning the precursor description, it is known that large PAHs are at the origin of soot nucleation. This role is fulfilled in the present model by naphthalene which is generally considered as a tracer for soot precursors. It also yields a good estimate of soot volume fractions f_v in laminar premixed flames. However, this may not be the case in the turbulent flame configuration where other soot production processes may intervene.

More specifically, an examination of the spatial localization of the source terms in the laminar flame (Fig. 4) indicates that oxidation mainly occurs in the early-stage soot formation since OH mass fraction (Fig. 5) appears close to the flame front. Thus, soot oxidation plays a negligible role in laminar premixed flames. This conclusion has been verified also at higher equivalence ratios (not shown). A different behaviour is observed in the EM2soot burner. Similar to the laminar flames, the oxidation process is localized in a small region (mainly related to OH presence), close to the injection, i.e. in the flame front region, whereas nucleation and condensation occur downstream, i.e. in the IRZ where A_2 is mainly produced. Still, due to the recirculation, the newly produced particles are pushed towards the injector where surface growth and oxidation occur. Thus, in the EM2Soot burner the oxidation process attaints maximum values higher than nucleation and of the same order as condensation, i.e. oxidation may play a significant role in this configuration. Thus, the overestimation of f_v in the EM2Soot burner may be due to an underestimation of the oxidation process. This may be verified by examining the impact of a model in which oxidation is enhanced.

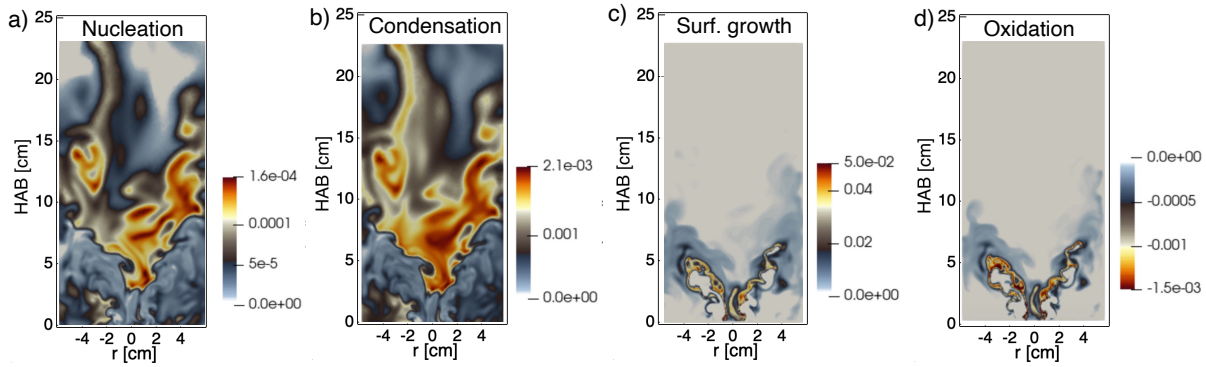

Figure 6: Instantaneous 2D fields of soot mass production rate (in Kg/m^3/s) for the EM2Soot burner using the reference oxidation model.

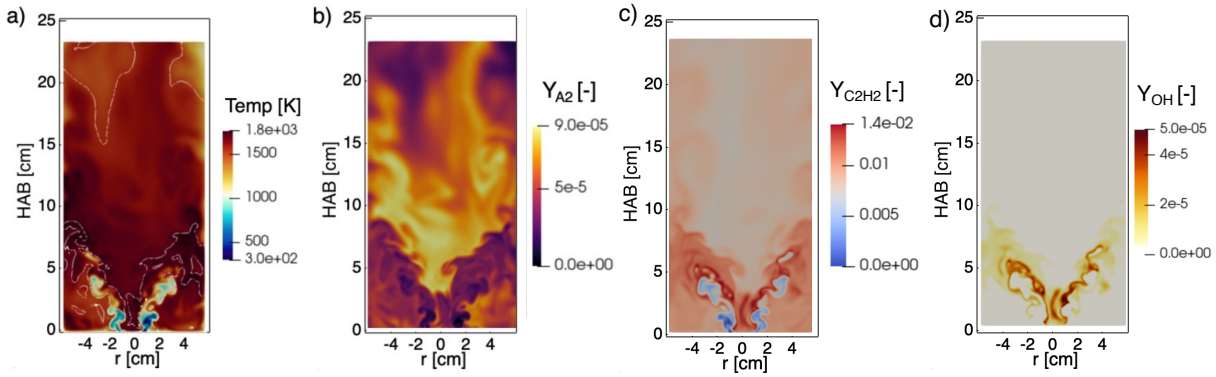

Figure 7: Instantaneous 2D fields of temperature and species mass fractions for the EM2Soot burner using the reference oxidation model. White isocontours of A_2 mass fraction equal to $Y_A2 = 4.0e^{-5}$ are superimposed to the temperature field.

Impact of an augmented oxidation rate model

To examine the role of the oxidation model the oxidation source terms are augmented by a factor of 10 in the laminar and turbulent flame cases. There are no significant differences between the reference and the augmented oxidation rate (AOR) models in the laminar flame case (Fig. 8). The f_v values obtaind with the AOR model at a height HAB=15 mm are close to those obtained with the reference scheme (Fig. 8).

This confirms that the oxidation process has only a minor influence in rich premixed laminar flames (at least for the models retained in this work).

In the EM2Soot case, the simulation has been performed over 70 ms starting from the final solution of the reference oxidation scheme. This computational time is far from being sufficient to reach the steady solution for f_v and the simulation is still ongoing. Still, the instantaneous f_v field shown in Fig. 9 already feature a significant decrease in the f_v level. This highlights the role of the oxidation process in the EM2Soot burner where the turbulent flow features large scale recirculating eddies. The flow organization in combination with the oxidation kinetics are seen to determine the soot level. This indicates that it is valuable to test soot models under turbulent conditions.

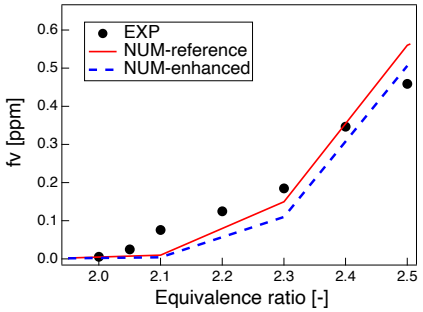

Figure 8: **C**omparison between experimental [20] (symbols) and numerical f_v for ϕ at a distance of 15 mm from the flame front with the reference (continuous) and the enhanced (dashed) oxidation model in a laminar premixed flame at ambient temperature and atmospheric pressure for different ϕ.

Conclusions

Calculations reported in this article rely on a LES to model soot formation in rich premixed turbulent flames. This numerical framework suitably retrieves soot volume fraction (SVF) levels in rich premixed laminar flames. In the turbulent flame case, it reproduces the SVF trend as function of the equivalence ratio as well as the SVF spatial distribution, but the predicted levels are

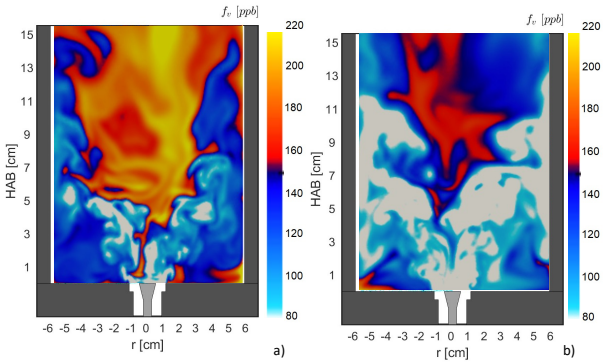

Figure 9: Comparison between reference (a) and augmented (b) instantaneous SVF at reference conditions [12].

notably overestimated with respect to the experimental results. An extensive analysis of the flame structure as well as of the soot source terms indicates that this is possibly due to an underestimation of soot oxidation reactions and to an imperfect description of the oxidation processes taking place in the post-flame region. A tuning of the soot kinetic model consisting in augmenting the oxidation rates of reaction by an order of magnitude with respect to the standard values of these rates is shown to have no impact in the rich premixed laminar flame case but yields a significantly lower SVF in the rich premixed turbulent flame case that comes closer to the values determined experimentally. This result, obtained with an admittedly empirical tailoring of the soot oxidation rates, indicates that it is worth testing the soot models in turbulent flame configurations to reveal some of their shortcomings and to obtain insights on the processes that need to be revisited. In this respect, the rich premixed turbulent flame EM2Soot system constitutes an instructive testbed that is realistic but sufficiently simple to obtain useful information on soot formation and oxidation processes. Future studies will include the analysis of the influence of an improved oxidation model over a wider range of laminar and turbulent flames to further assist the development of new oxidation models.

Acknowledgements

This project has received the support of the European Research Council (ERC) under the European Union's Horizon 2020 research and innovation programme (Grant Agreement No. 757912). The work was performed using HPC resources from the "Mésocentre" computing center of Centrale Supélec and École Normale Supérieure Paris-Saclay supported by CNRS and Région Île de-France and the HPC resources from GENCI-CINES (Grants 2021-A0112B12029 and 2022-A0132B12029). We thank CERFACS for kindly sharing the AVBP solver with us and L. Gallen, E. Riber and B. Cuenot from CERFACS for sharing the C2H4_28_205_14_LG scheme.

References

[1] A. C. Brown, in *Transport and Clean Air Seminar* (2013).

[2] J. Lelieveld, K. Klingmüller, A. Pozzer, U. Pöschl, et al., *European Heart Journal* **40**, 1590 (2019).

[3] K. P. Geigle, R. Hadef, and W. Meier, *Journal of Engineering for Gas Turbines and Power* **136** (2013).

[4] M. Bouvier, G. Cabot, J. Yon, and F. Grisch, *Proceedings of the Combustion Institute* **38**, 1851 (2021).

[5] I. El Helou, A. W. Skiba, and E. Mastorakos, *Flow, Turbulence and Combustion* **106**, 1019 (2021).

[6] I. A. Mulla and B. Renou, *Combustion and Flame* **209**, 452 (2019).

[7] B. Franzelli, L. Tardelli, M. Stöhr, K. P. Geigle, and P. Domingo, *Proc Combust Inst* (2022).

[8] L. Tardelli, N. Darabiha, D. Veynante, and B. Franzelli, *Proceedings of ASME TurboExpo 2021, GT2021-60296* (2021).

[9] M. Grader, Z. Yin, K. P. Geigle, and P. Gerlinger, *Proceedings of the Combustion Institute* **38**, 6421 (2021).

[10] S. T. Chong, M. Hassanaly, H. Koo, M. E. Mueller, V. Raman, and K. P. Geigle, *Combustion and Flame* **192**, 452 (2018).

[11] L. Gallen, A. Felden, E. Riber, and B. Cuenot, *Proceedings of the Combustion Institute* **37**, 5429 (2019).

[12] A. Maffina, M. Roussillo, P. Scouflaire, N. Darabiha, D. Veynante, S. Candel, and B. Franzelli, *Proceedings of ASME TurboExpo 2023, GT2023-104174* (2023).

[13] M. Roussillo, Ph.D. thesis, Université Paris-Saclay, Gif-sur-Yvette, France (2019), `https://theses.hal.science/tel-02317701`.

[14] M. Roussillo, P. Scouflaire, N. Darabiha, S. Candel, and B. Franzelli, in *Proceedings of the ASME Turbo Expo 2018: Turbomachinery Technical Conference and Exposition. Volume 4B: Combustion, Fuels, and Emissions* (2018), V04BT04A006.

[15] L. Gallen, Ph.D. thesis, Université de Toulouse, Toulouse, France (2020), `https://www.theses.fr/2020INPT0058`.

[16] M. Thomson and T. Mitra, *Science* **361**, 978 (2018).

[17] M. Frenklach and H. Wang, *Symposium (International) on Combustion* **23**, 1559 (1991).

[18] B. Franzelli, A. Vié, and N. Darabiha, *Proceedings of the Combustion Institute* **37**, 5411 (2019).

[19] J. Smagorinsky, *Monthly Weather Review* **91**, 99– (1963).

[20] R. Hadef, K. P. Geigle, W. Meier, and M. Aigner, *International Journal of Thermal Sciences* **49**, 1457 (2010).